Mps1 promotes chromosome meiotic chromosome biorientation through Dam1

Régis E. Meyer[a], Jamin Brown[a], Lindsay Beck[a], and Dean S. Dawson[a,b,*]
[a]Program in Cell Cycle and Cancer Biology, Oklahoma Medical Research Foundation, and [b]Department of Cell Biology, University of Oklahoma Health Sciences Center, Oklahoma City, OK 73104

ABSTRACT **In budding yeast meiosis, homologous chromosomes become linked by chiasmata and then move back and forth on the spindle until they are bioriented, with the kinetochores of the partners attached to microtubules from opposite spindle poles. Certain mutations in the conserved kinase, Mps1, result in catastrophic meiotic segregation errors but mild mitotic defects. We tested whether Dam1, a known substrate of Mps1, was necessary for its critical meiotic role. We found that kinetochore–microtubule attachments are established even when Dam1 is not phosphorylated by Mps1, but that Mps1 phosphorylation of Dam1 sustains those connections. But the meiotic defects when Dam1 is not phosphorylated are not nearly as catastrophic as when Mps1 is inactivated. The results demonstrate that one meiotic role of Mps1 is to stabilize connections that have been established between kinetochores and microtubles by phosphorylating Dam1.**

Monitoring Editor
Kerry S. Bloom
University of North Carolina

Received: Aug 9, 2017
Revised: Dec 1, 2017
Accepted: Dec 7, 2017

INTRODUCTION

During meiosis, cells face a critical transition from a stage where chromosomes are dispersed, and unattached to microtubules (prophase), to a stage where paired homologous partners are aligned on the middle of the spindle (metaphase). This transition starts with the capture of chromosomes by the spindle microtubules resulting in mostly incorrect initial attachments. If uncorrected, these kinetochore–microtubule (kMT) attachments would pull the homologous partners to the same pole rather than to opposite poles of the spindle at anaphase (Meyer *et al.*, 2013). These aberrant attachments are corrected to avoid mis-segregation and aneuploidy (reviewed in Duro and Marston, 2015). In yeast meiosis, the correction is done via consecutive cycles of deattachment/reattachment of microtubules to the kinetochores, accompanied by movements of the chromosomes back and forth on the spindle as they orient (Meyer *et al.*, 2013). During this process, the spindle assembly checkpoint senses the state of kMT attachments and delays cell cycle progression into anaphase until all chromosome pairs are bioriented (Hoyt *et al.*, 1991; Li and Murray, 1991; Cheslock *et al.*, 2005; Shonn *et al.*, 2000; reviewed in Joglekar, 2016). When the spindle assembly checkpoint is satisfied, anaphase ensues.

A key aspect of the chromosome biorientation process involves modulating the type and the stability of kMT attachments depending on chromosome position. The kMT attachment process appears to be controlled at several levels (reviewed in Tanaka, 2010; Godek *et al.*, 2015; and Lampson and Grishchuk, 2017). In yeast, this has been studied primarily in mitotic cells. First, new attachments must be formed. In yeast, as in other organisms, kinetochores initially attach most often to lateral surfaces of microtubules (Hayden *et al.*, 1990; Merdes and De Mey, 1990; Rieder, 1990; Tanaka *et al.*, 2005; Franco *et al.*, 2007; Gachet *et al.*, 2008; Magidson *et al.*, 2011). Second, when depolymerization of the microtubule brings the end of the microtubule to a laterally attached kinetochore, the connection can be converted to an end-on attachment (Kitamura *et al.*, 2007; Tanaka *et al.*, 2007). Third, the protein composition at the kMT interface, and modifications of those proteins, change, which promotes the ability of the kinetochore to track the shortening microtubule (Asbury *et al.*, 2006; Westermann *et al.*, 2006; Grishchuk *et al.*, 2008; Daum *et al.*, 2009; Gaitanos *et al.*, 2009; Powers *et al.*, 2009; Welburn *et al.*, 2009; Lampert *et al.*, 2010; Schmidt *et al.*, 2012; Volkov *et al.*, 2013; Umbreit *et al.*, 2014). Finally, incorrect connections that do not promote biorientation are released (Biggins *et al.*, 1999; Cheeseman *et al.*, 2002; Tanaka *et al.*, 2002).

Mps1 is a conserved kinase with a central role in the spindle assembly checkpoint (Hardwick *et al.*, 1996; Weiss and Winey, 1996;

This article was published online ahead of print in MBoC in Press (http://www.molbiolcell.org/cgi/doi/10.1091/mbc.E17-08-0503) on December 13, 2017.
*Address correspondence to: Dean S Dawson (dawsond@omrf.org).
Abbreviations used: kMT, kinetochore–microtubule; SPB, spindle pole body.

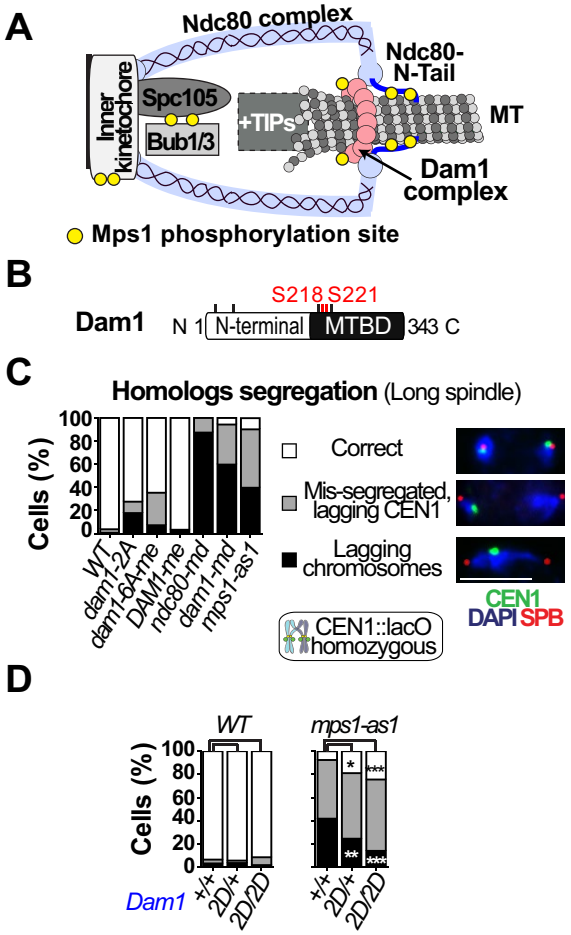

FIGURE 1: Dam1 phosphorylation promotes meiotic segregation. (A) Cartoon highlighting the distribution of proteins known to be phosphorylated by Mps1 kinase at the kMT interface (Cnn1 is the target for the inner kinetochore). Ndc80, Dam1, and Spc105 represent sub-complexes composed of two or more proteins (reviewed in Biggins, 2013). +TIPs indicates microtubule plus-end tracking proteins such as Stu1, Stu2, and Bim1 (not necessarily in the same location or exactly at the frayed end of the microtubule). The proteins shown are not necessarily at the kMT interface at the same time. Yellow circles indicate known Mps1 phosphorylation sites. (B) Domains of Dam1 protein. Known residues phosphorylated by Mps1 in budding yeast are represented by black lines. (C, D) All strains evaluated were diploids with GFP-tagged centromeres of chromosome 1 (CEN1-GFP) and expressing *SPC42-DsRed* to mark the SPBs. Cells were sporulated and released from a pachytene arrest (P_{GAL1}-*NDT80 GAL4-ER*) at 6 h after meiotic induction by the addition of 5 μM β-estradiol. In the diploid cells with long spindles (length ≥ 3.5 μm), the proportion of cells exhibiting proper *CEN1* segregation (white), defective segregation of *CEN1* (gray), or numerous lagging chromosomes as observed by DAPI staining (black) was monitored 3-4 h postrelease ($n \geq 100$). An example of each category is shown. Scale bar: 5 μm. (C) Relevant genotypes of tested strains: *WT* is wild-type for *DAM1*, *NDC80*, and *MPS1*. *dam1-2A* is *dam1-2A/dam1-2A*, and *DAM1-me* is *DAM1-md/DAM1-me*, so meiotic production of Dam1 protein comes from the meiotic *IME2* promotor. *dam1-6A-me* is *DAM1-md/dam1-6A-me*, so expression of Dam1-6A protein comes from the meiotic *IME2* promotor. *ndc80-md* is P_{CLB2}-*NDC80*/ P_{CLB2}-*NDC80*. *dam1-md* is P_{CLB2}-*DAM1*/P_{CLB2}-*DAM1*. *mps1-as1* is *mps1-as1*/ P_{CLB2}-*MPS1* so meiotic expression of Mps1 is from the *mps1-as1* allele. For *mps1-as1* diploid mutants, 1 h after this release ($t = 7$ h), an inhibitor of the analog-sensitive allele *mps1-as1* (1NM-PP1, 10 μM) was added to the medium. (D) The *dam1-2D* allele expresses a protein in which two serines of Dam1 that are phosphorylated by Mps1 (S218 and S221) have been switched to aspartic acid. *$p < 0.05$, **$p < 0.01$, ***$p < 0.001$ (Fisher's exact test) ($n \geq 59$).

Abrieu *et al.*, 2001). In budding yeast meiosis, Mps1 performs an essential function in promoting the formation, maintenance, or regulation of force-generating attachments to the plus ends of microtubules (Meyer *et al.*, 2013). This seems to contradict the emerging picture of Mps1 function in mammalian mitotic chromosome biorientation, where Mps1 acts in part to destabilize kMT attachments (Jelluma *et al.*, 2010; Hiruma *et al.*, 2015; Ji *et al.*, 2015; Maciejowski *et al.*, 2017). In both yeast and mammals, Mps1 binds to the Calponin homology domain of the outer kinetochore protein, Ndc80 (Kemmler *et al.*, 2009; Nijenhuis *et al.*, 2013). In mammalian cells, Mps1 is displaced from the kinetochores chromosomes once they have become bioriented. Evacuation of Mps1 from the attached kinetochores contributes to turning off the spindle checkpoint "wait" signal (Etemad and Kops, 2016). The binding of microtubules to Ndc80 may displace or prevent Mps1 binding to Ndc80 (Hiruma *et al.*, 2015; Ji *et al.*, 2015). In budding yeast mitosis, tethering Mps1 to kinetochores does not result in a dramatic loss of kMT attachments as it does in mammalian cells (Aravamudhan *et al.*, 2015), consistent with the finding that Mps1 promotes, rather than destabilizes, kMT attachments in budding yeast meiosis.

The manner in which Mps1 promotes force generating attachments between kinetochores and microtubule plus-ends in meiosis is unclear. *MPS1* mutations have been described that result in catastrophic errors in meiotic chromosome segregation, but only mild mitotic defects, demonstrating there is a greater need for Mps1 in meiosis than in mitosis, but what that need might be is unknown. One way that Mps1 is known to impact the kMT interface in mitosis is through phosphorylation of Dam1 (Figure 1A). Dam1 is a member of the Dam1 complex, which interacts with the Ndc80 complex and increases its ability to hold on to microtubule plus ends in vitro (Franck *et al.*, 2007; Tien *et al.*, 2010; Lampert *et al.*, 2013; Sarangapani *et al.*, 2013). Two proteins of the Dam1 complex, Dam1 and Duo1, interact directly with microtubules (Asbury *et al.*, 2006; Westermann *et al.*, 2006; Zelter *et al.*, 2015). The Dam1 protein contains six residues that are phosphorylated by Mps1 (Figure 1B) (Shimogawa *et al.*, 2006). Prior work has shown that mutation of two of these residues (serine 218 and 221) to nonphosphorylable amino acids results in diminished levels of end-on attachments in mitotic yeast cells (Shimogawa *et al.*, 2006; Shimogawa *et al.*, 2010), suggesting that Mps1 might promote the formation or maintenance of end-on attachments thru Dam1. Despite the fact that *dam1-2A* (S218A S221A) mutants have reduced end-on kMT attachments, they only exhibit minor mitotic chromosome segregation defects, suggesting that normal end-on kMT attachments might not be essential for effective mitotic chromosome segregation in budding yeast. The severe defects of some *MPS1* mutants in meiosis, but not mitosis, raises the question of the meiotic consequences of Dam1 phosphorylation by Mps1.

RESULTS

Mps1 works partially through Dam1 to promote meiotic chromosome segregation

To better understand how Mps1 controls meiotic poleward chromosome movement, and how Dam1 might be involved, we analyzed meiotic chromosome movements in *dam1* mutants. We assayed both the *dam1-2A* allele, described above, and a *dam1-6A* allele in

which all the Mps1 phosphorylation sites were converted to alanines. To prevent the accumulation of potential mitotic errors, the *dam1-6A* allele was placed under control of a promotor (P_{IME2}) that is turned off in mitotic growth but is meiotically expressed (*me*) (*dam1-6A-me*). The other *DAM1* allele was wild type, but under the control of the *CLB2* promotor that is expressed only in mitotic cells, resulting in meiotic depletion (md) (*DAM1-md*) (Lee and Amon, 2003). Because the Dam1 protein is degraded on meiotic entry and Dam1 complexes are reassembled prior to metaphase I (Miller *et al.*, 2012; Meyer *et al.*, 2015), the *DAM1-md/dam1-6A-me* combination allows us to assay the effect of preventing Mps1 phosphorylation of Dam1 in meiosis. The segregation of a green fluorescent protein (GFP)-tagged version of chromosome I was monitored in cells harvested from meiotic time courses to assay the effects of the *dam1* mutants. The *dam1-2A* and *-6A* alleles exhibited similar increases in meiosis I nondisjunction and lagging chromosomes suggesting that the critical residues are the serines mutated in *dam1-2A* mutants (S218 and S221) (Figure 1C). The lagging chromosomes were mainly associated with metaphase spindles (Supplemental Figure S1A) rather than anaphase spindles (as seen in *mps1* null mutants) (Meyer *et al.*, 2013). Depletion of Dam1 (*dam1-md*) had catastrophic defects (Figure 1C) similarly to what was observed when cells were depleted for the essential outer kinetochore protein Ndc80 (*ndc80-md*). The *dam1-md* allele also resulted in failures of meiotic spindle integrity (Supplemental Figure S1B) similarly to what was reported for *dam1* null mutants in mitosis (Jones *et al.*, 1999).

These defects of the nonphosphorylatable *dam1* mutants were much less severe than the defects of *mps1-as1* mutants (Figure 1C), demonstrating that Dam1 is not the most critical target of Mps1 in meiotic biorientation. But to test whether the meiotic segregation defects exhibited by *mps1* mutants might be partially attributable to a failure to phosphorylate Dam1, we introduced a version of *DAM1* with phosphomimetic mutations (S218D, S221D; *dam1-2D*) into *mps1-as1* mutants (Figure 1D). The *dam1-2D* allele improved segregation fidelity in these strains, suggesting that the severe failure of meiotic chromosome segregation in *mps1* mutants is partially attributable to a failure to phosphorylate Dam1. Less clear are the specific contributions that phosphorylating Dam1 makes to the biorientation process.

Phosphorylation of Dam1 by Mps1 stabilizes associations of centromeres with the microtubules

Live cell imaging was used to determine whether the *dam1-2A* mutation affected chromosome movements during the biorientation process. The experiment was performed in a *spo11* mutant background in which chromosomes do not become tethered to their homologous partners. In this situation, the resulting individual (univalent) chromosomes, each with one kinetochore, can only attach to a single microtubule (Figure 2A). Thus, they can never biorient, resulting in repeated cycles of forming kMT attachments, chromosome movement toward the poles, and release of the kMT attachment (Figure 2B) (Meyer *et al.*, 2013). The *spo11* mutation also results in a longer spindle, making it easier to track long processive movements of chromosomes (Shonn *et al.*, 2000; Meyer *et al.*, 2013). Using this assay, *dam1-md* mutants exhibit a nearly complete loss in the ability of chromosomes to traverse the spindle, while *dam1-2A* mutants are significantly compromised in the process (Figure 2, C and D, and Supplemental Figure S2). A similar, but less severe, deficiency was observed for *dam1-2A* mutants when the behavior of bivalent pairs (*SPO11* background) was evaluated in this type of assay (Supplemental Figure S3, A–G). The shorter spindles and the availability of two connected kinetochores to which

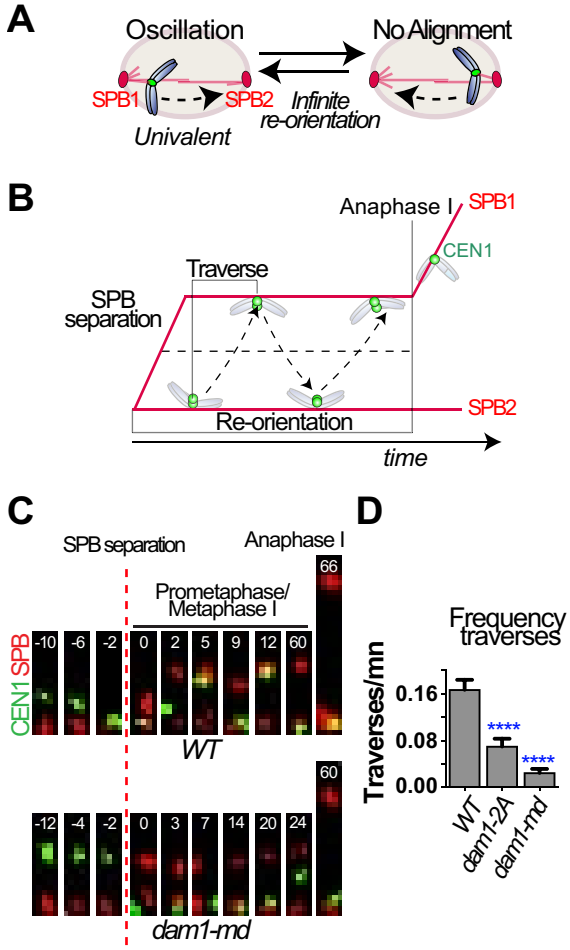

FIGURE 2: Phosphorylation of Dam1 by Mps1 promotes processive migration on the meiotic spindle. (A) Cartoon illustrating the process of reorientation in the absence of links between homologues (*spo11*Δ background). As the univalent does nt have the ability to biorient, it will reorient indefinitely. (B) The reorientation process in the *spo11* background can be evaluated by quantifying the traverses. (C, D) *spo11*Δ diploid cells, with the indicated genotypes, with one GFP-tagged *CEN1* and the SPB marker (*SPC42-DsRed*) were sporulated and released from a pachytene arrest (P_{GAL1}-*NDT80 GAL4-ER*) at 6 h after meiotic induction by the addition of 5 μM β-estradiol. The cells were observed by a time-lapse movie at 45-s intervals for 75 min. A representative series of images from wild-type and *dam1-md* mutant cells are shown. (D) Strain genotypes are as in Figure 1. The number of CEN1-GFP traverses per minute during the first 20 min following spindle formation was determined in individual cells. ****$p < 0.0001$ (Student's *t* test) ($n \geq 18$).

microtubules can attach may explain why the *dam1-2A* defect in across-the-spindle traverses is less severe in the *SPO11* strain.

The coupling of kinetochores to the ends of depolymerizing microtubules is presumably the major driving force for the poleward movements that occur on bipolar spindles. However, in assays with bipolar spindles (as in Figure 2C), it is difficult to know exactly how the kinetochore of a particular chromosome is attached to a microtubule. To measure more specifically minus-end directed movements, we assayed the clustering of a univalent chromosome (*spo11* background) toward the side-by-side spindle pole body (SPBs) before the bipolar spindle is formed (Figure 3A). Because the microtubules form a monopolar array, all poleward movements are

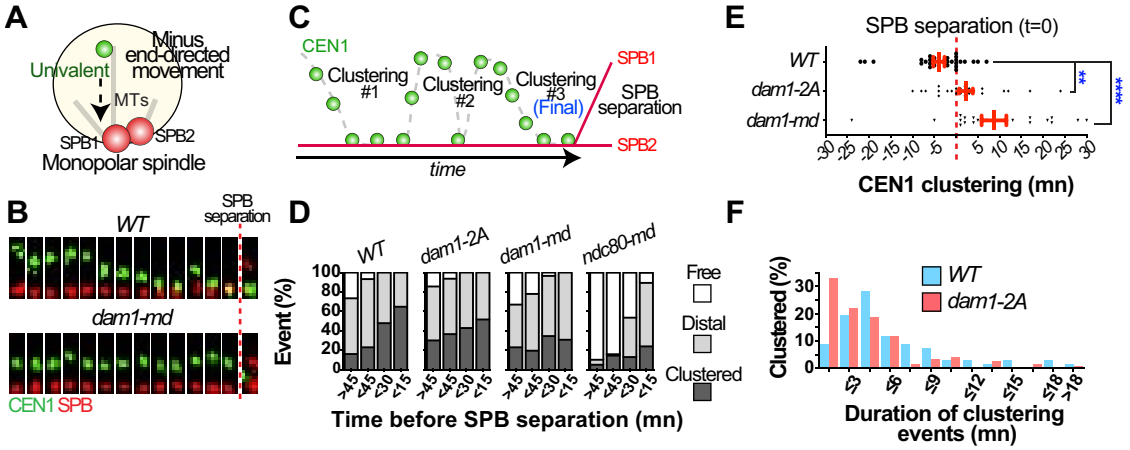

FIGURE 3: Dam1 phosphorylation promotes stable pulling forces on monopolar microtubule arrays. (A) Schematic representation of centromere clustering on a monopolar microtubule array. Tracking the relative distance between an individual chromosome and the unseparated SPBs can monitor this process. (B–F) *spo11*Δ diploid cells (from Figure 2, A–D) were imaged at 45-s intervals for 75 min. (B) Representative wild-type or *dam1-md* mutant cells showing the behavior of a centromere leading up to spindle formation (the last frame shown after the dotted line). (C) The pulling of the chromosome can be separated in two alternating phases where *CEN1* is either moving toward the SPBs (Clustering) or at a relative constant distance from the SPBs. (D) The status of *CEN1* was monitored, at each interval, for each individual cell, of the indicated genotypes and classified as follows: Free (white) when the relative position of *CEN1* to the SPBs was unstable (moving closer and farther from the SPBs in consecutive frames), distal (gray) when *CEN1* was more than 0.5 µm from the SPBs and staying at a constant distance or moving incrementally closer or farther from the SPBs in consecutive frames and clustered (dark gray), when *CEN1* was staying close (less than 0.5 µm from the SPBs). We assume that most "distal" and "clustered" *CEN1*s are attached to microtubules and "free" *CEN1*s are not. The proportion for each class in each period of 15 min preceding bipolar spindle formation is shown ($n \geq 10$ cells). (E) The timing of the final clustering of *CEN1* was monitored relative to SPB separation for each individual cell of the indicated genotypes ($n \geq 19$). The red dotted line represents the time at which SPBs separated. $^{**}p < 0.01$, $^{****}p < 0.0001$ (Student's *t* test). (F) From D the duration of each clustering event was monitored (number of minutes *CEN1* stayed within 0.5 of the SPBs. The distribution of those events in the wild-type and *dam1-2A* mutant cells (67 vs. 118 events, respectively) is shown. The average time spent clustered in *dam1-2A* cells was significantly less than in *WT* (unpaired *t* test, $p = 0.0048$).

minus-end directed. Following the release from a prophase arrest, the univalents migrate toward the side-by-side SPBs (cluster) in consecutive cycles (Figure 3, B and C). In wild-type cells, the clustering events were more and more frequent approaching the time of spindle formation (Figure 3D), leading to a final clustering several minutes before the SPBs separated to form a spindle (Figure 3E). The *dam1* mutants show significant delays in reaching the final clustering (Figure 3E). Similar observations were obtained by monitoring bivalent pairs (*SPO11*) (Supplemental Figure S3, H and I).

The delay in clustering in *dam1-2A* mutants could reflect a deficiency in minus-end-directed movement or a failure in remaining at the SPBs once they have arrived. Indeed, in the *dam1-2A* mutants, centromeres spent less time at the SPBs before migrating away again (Figure 3F), suggesting the phosphorylation of Dam1 by Mps1 stabilizes the association of the centromeres with the SPBs, perhaps by stabilizing the kMT attachment.

dam1 mutants exhibit pausing defects during the biorientation process

The imaging experiments above employ long acquisition interval times (2 min/frame) to allow acquisition of data for cells proceeding from prometaphase thru anaphase I, without photobleaching or toxicity. At this frame rate, a traverse across the entire spindle can occur in the interval between sequential frames. To reveal the pauses and restarts to chromosome movement that might occur within a single traverse, we imaged chromosome behavior at faster acquisition rates (2 s intervals) over the course of 5 min. Images were acquired using a thru-focus method in which a single image is collected as the objective lens focuses thru the cell (Conrad *et al.*, 2008). Deconvolution of the acquired data produces a two-dimensional projection of the image. To reduce acquisition times, the SPBs and the centromere of chromosome I were both tagged with GFP.

Chromosome behavior was quantified in cells with bipolar spindles. In the control wild-type (*WT*) cells, chromosomes were found to exhibit any one of several different behaviors during the 5-min filming. We assigned the behaviors to five categories (Figure 4A). These included high-mobility traverses across all of or part of the spindle, pausing at the pole, pausing in a nonpolar area—either midspindle, or to the side of the line between the two spindle pole bodies—and limited movements in a small area (low mobility) (Figure 4A). Whereas visualizing the chromosomes undergoing high-mobility movements across part of the spindle (trials) or the whole spindle (traverses) was common in the control strain, this was less common in *dam1-2A* and *dam1-md* mutants. In contrast, whereas it was uncommon in the control strain for chromosomes to exhibit centromeres that lingered in a nonpolar position, this was a predominant behavior in the *dam-1-md* strain (Figure 4, B–D). In the *dam1* mutants, the nonpolar centromeres moved around much like centromeres in nonpolar positions in wild-type cells (Figure 4, B–D). In fact, centromeres that remained in a nonpolar position in the WT, *dam1-2A*, and *dam1-md* strains behaved in an indistinguishable manner, the main difference being that this phenotype was much more common in the *dam1-md* strain. One possible explanation is

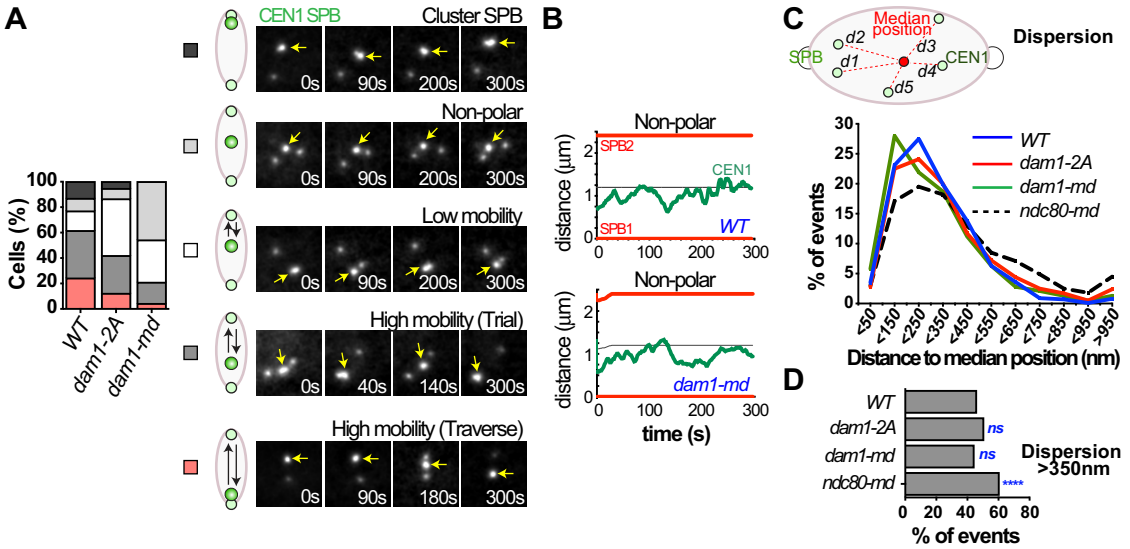

FIGURE 4: Phosphorylation of Dam1 by Mps1 promotes chromosome mobility on the meiotic spindle. In *spo11*Δ diploid cells, with the indicated genotypes, one *CEN1-GFP* tagged chromosome and a SPB marker (*SPC42-GFP*) were sporulated and released from a pachytene arrest (P_{GAL1}-*NDT80 GAL4-ER*) at 6 h by the addition of 5 µM β-estradiol. Cells were observed by time-lapse imaging during meiosis at 2-s intervals for 5 min. (A) Cells were placed in categories according to the behavior of *CEN1*. Cells that exhibited one or more complete spindle traverses or shorter trials were put in one of those categories. Other cells were classified as low mobility if they showed smaller movements, or midspindle or clustered, if *CEN1* primarily stayed in one of those positions. Examples of each classification are shown. (B) Representative kymographs of cells from three different genotypes that were classified as "nonpolar." (C) Movement of nonpolar centromeres. For centromeres classified as nonpolar, we calculated the median position of *CEN1* over the course of the 5-min imaging period and then the distance of *CEN1* from that median position for each frame of the acquisition. The graph shows the relative distribution of distances measured for each genotype ($n \geq 750$ for each genotype). (D) The proportion of individual *CEN1* positions more than 350 nm distant from the median position was calculated for each indicated genotype. Mutant genotypes were compered to *WT*. ****$p < 0.0001$ (Fisher's exact test) ($n \geq 750$).

that in the *dam1* mutants, the kinetochores are less able to efficiently secure microtubule attachments, so they spend more time uncoupled from microtubules and less time undergoing high-mobility, microtubule-mediated movements. But in *ndc80* mutants, in which kinetochores are presumably unattached to microtubules, the centromeres in a nonpolar position showed somewhat more movement than was seen in *dam1-md, dam1-2A,* and wild-type cells. It may be that without connections to microtubules, the centromeres in *ndc80* mutants are mobilized by the much faster meiotic telomere-led movements (Conrad *et al.*, 2008). Thus, we speculate that the midspindle centromeres in WT, *dam1-md,* and *dam1-2A* are undergoing some microtubule interactions and these interactions impact their movement.

dam1 exhibit reduced processivity during poleward centromere migrations

The *dam1-2A* results suggest the model that phosphorylation of Dam1 by Mps1 in meiosis promotes either the establishment or maintenance of kMT attachments, consistent with observations in mitotic cells (Shimogawa *et al.*, 2006). To attempt to distinguish between these models, we characterized the behavior of centromeres making poleward migrations in wild-type and *dam1-2A* cells. We identified centromeres that moved from a position of 1 micron away from a spindle pole to the pole (Figure 5A). These movements toward a pole could come from either pushing or pulling forces, but since the migrations occur within one half spindle (average spindle length was more than 2 microns), they are presumably mediated most often by minus-end-directed movements along a microtubule that emanates from the destination pole. These poleward migrations took significantly less time in wild-type cells than in *dam1-2A* mutants (Figure 5, B and C). To determine whether this was because centromeres reach higher velocities in wild-type cells, we measured the distance that each centromere moved over each frame (2 s) of acquisition (Figure 5D) for both poleward and anti-poleward centromere movements that occurred over the course of migration to the pole. There was no significant difference in the velocities of the centromeres in the two strains. The peak movement at ~45 nm/s translates to 2.7 µm/min, which is close to the previously published rate at which plus-end-attached mitotic kinetochores move on depolymerizing microtubules (1.5–2.0 µm/min; Gandhi *et al.*, 2011). The slightly faster rate, observed here, is likely due to the fact that we are reporting movement over 2-s intervals while previous reports represent the average speed over longer time intervals that probably included short pauses (as in the migrations plotted in Figure 5B). The fact that centromeres *dam1-2A* mutants are able to move at the same maximal velocity as in wild-type cells is consistent with the model that force-generating, end-on microtubule attachments can be formed without Mps1 phosphorylation of Dam1.

What did differ between the WT and *dam1* strains is the processivity of movement toward the pole (Figure 5, E–G). The *dam1* mutants exhibited more pauses, or reversals of direction, in their journeys to the pole (Figure 5, F and G).

dam1-2A mutants cannot maintain midspindle biorientation

A possible explanation for the frequent pauses and reversals of poleward migrating univalents in *dam1-2A* mutants is that the force exerted on the kinetochores of poleward migrating

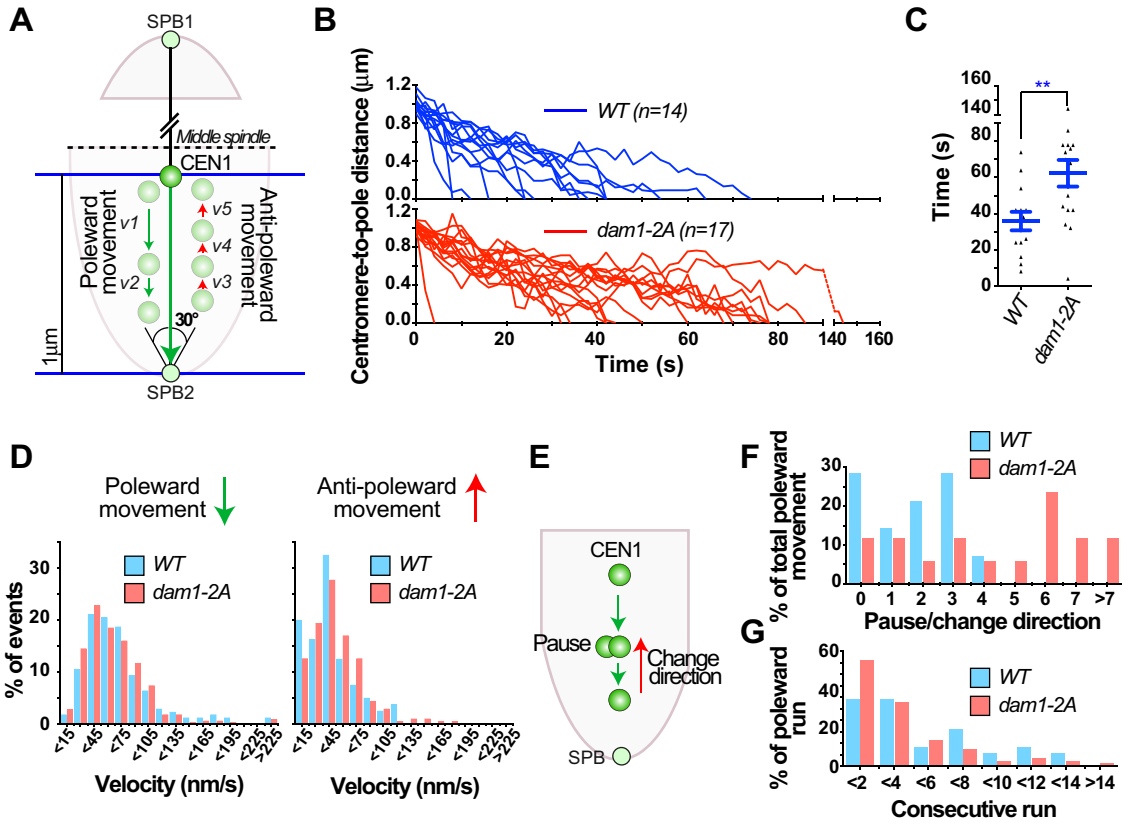

FIGURE 5: Dam1 phosphorylation promotes processive poleward movement. (A) We identified cells in which *CEN1* migrated across midspindle to the pole along the central axis of the spindle (within 15° of the axis from the destination SPB). Movements for the final 1 µm of the migration were quantified. (B) Kymographs of the poleward movement for wild-type (blue) and *dam1-2A* mutants (red). $T = 0$ represents the time *CEN1* is 1 µm from the SPB. (C) Graph of the cells in B showing the time spent for each *CEN1* to reach the SPB from 1 µm away (bars represent average and standard error of the mean). $^{**}p < 0.01$ (Student's *t* test). (D) Distribution of the velocities of the incremental poleward (left) or anti-poleward (right) *CEN1* movements measured during the 1-µm poleward movement. The velocities reflect the distance traveled by *CEN1* in one frame (2 s). Poleward and anti-poleward velocities were determined by analyzing the movement with respect to the (decreasing or increasing) distance between *CEN1* and the destination SPB. (E) Cartoon illustrating the pause or change of direction of *CEN1* movement than can happen during a 1-µm poleward migration. (F) For each individual 1-µm poleward migration, the number of pauses or changes of direction was determined. The graph shows the percentage of cells of each genotype with a given number of pauses/changes per 1-µm migration. Average pauses per migration and difference from the wild-type control (Student's *t* test) were as follows: *WT* 1.7 ± SEM 0.37, $n = 14$; *dam1-2A* 4.3 ± 0.67, $n = 17$, $p < 0.005$. (G) For each migration, the number of consecutive frames in which *CEN1* moved poleward without a pause or reversal was tabulated and graphed. The average number of consecutive poleward frames without pausing and difference from the wild-type control (Student's *t* test) were as follows: *WT* 5.37 ± SEM 0.59, $n = 38$; *dam1-2A* 3.85 ± 0.34, $n = 98$, $p < 0.05$.

univalents is sufficient to sever the kMT connection. In wild-type control cells, the kinetochores of bioriented chromosomes are positioned midspindle, with the centromeres alternating between being visibly separated or together (fused) (Figure 6A). Sometimes the centromere pair will migrate to one pole, generally with the centromeres in the fused configuration. Presumably, this reflects the loss of a connection between one kinetochore and its microtubule. As a first assessment of the ability of *dam1-2A* cells to maintain their kMT connections, we monitored the persistence of bioriented bivalents in the midspindle position (over long time periods with images collected at 2-min intervals; example traces for two cells are shown in Figure 6B). In *dam1-2A* mutants, the bivalents spent significantly less continuous time in a midspindle position (Figure 6C). Shorter acquisitions, with rapid frame rates (every 2 s for 10 min) were used to evaluate breathing of the centromeres of bioriented bivalents and the frequency with which they collapsed to a single pole with nonseparated centromeres. The breathing rate—the rate at which the centromeres of bioriented bivalents reseparated after coming together—was not dramatically different in *dam1-2A* and control cells (Figure 6D). Thus, kMT connections in control and *dam1-2A* mutants seem similarly able to generate tension across the bioriented kinetochores. However, in the *dam1-2A* mutants, the bioriented pair often lost their midspindle position and collapsed to one pole with unseparated centromeres (Figure 6E). If the collapse to one pole is because kMT attachments are unstable, then this should activate the spindle checkpoint. Indeed, when the spindle checkpoint is inactivated by deletion of the *MAD2* gene in the *dam1-2A* mutants they exhibit elevated rates on meiosis I nondisjunction (Supplemental Figure S4).

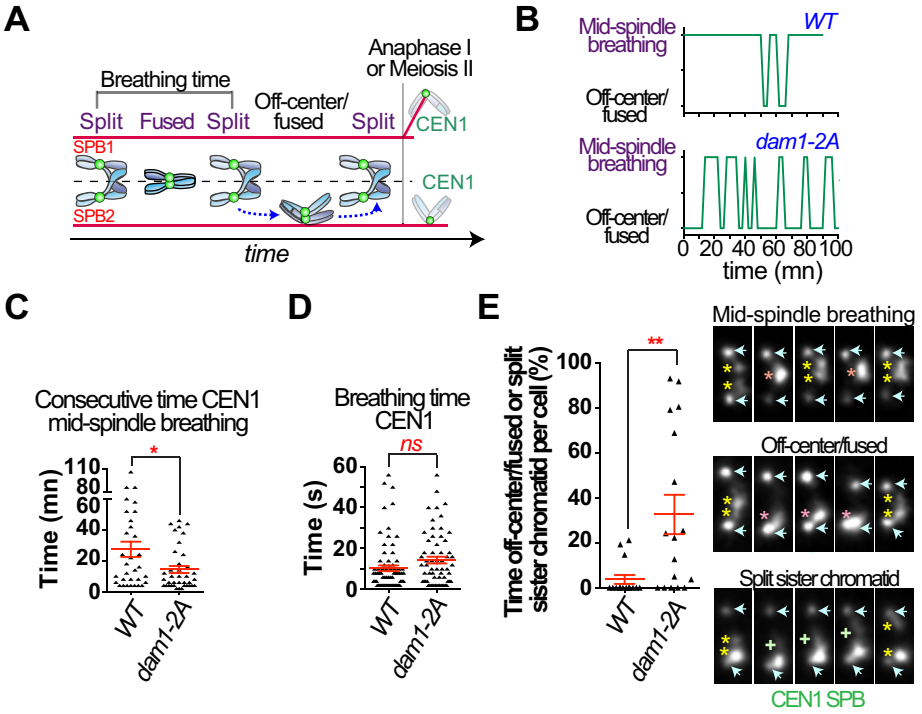

FIGURE 6: Dam1 phosphorylation stabilizes bioriented attachment. (A) Cartoon illustrating events occurring after establishment of a bioriented attachment until anaphase I onset. A bioriented bivalent alternates between phases in which the GFP-tagged centromeres appear as separate dots ("split") and phases in which the signals overlap ("fused"). The time between losing the split configuration and the next split configuration is defined as "breathing time." The bioriented bivalent sometimes moves off a midspindle position with a single centromere GFP signal. We defined this time to be "off-center fused." (B, C) The cells had GFP-tagged centromeres of chromosome 1 (CEN1-GFP) and expressed *SPC42-DsRed* to mark the SPBs. Cells were sporulated and released from a pachytene arrest (P_{GAL1}-*NDT80 GAL4-ER*) at 6 h after meiotic induction by the addition of 5 μM β-estradiol. Cells were imaged at 2-min intervals for 4 h. (B) Traces of the chromosomes in a single cell alternating between a midspindle breathing position and off-center fused position. Representative cells for the indicated genotype are shown. (C) For each cell, the time (total consecutive frames) spent with the configuration "Mid-spindle breathing" was determined. The graph represents their distributions for wild-type and *dam1-2A* mutant cells ($n \geq 32$). *$p < 0.05$ (Student's *t* test). (D, E) Diploid cells of the indicated genotype expressing homozygous *CEN1-GFP* and the SPB marker (*SPC42-GFP*) were sporulated and released from a pachytene arrest (P_{GAL1}-*NDT80 GAL4-ER*) at 6 h by the addition of 5 μM β-estradiol. A short-term time-lapse movie (2-sintervals for 10 min) was done. (D) The duration of each breathing event was determined and graphed ($n \geq 63$). ns = nonsignificant, $p > 0.05$ (Student's *t* test). (E) Time spent in each of the following configurations was scored: "midspindle breathing," "off-centered/fused," and "stretched or split sister chromatids." This last category was rare and appears as a less than full GFP signal pulled away from the main bright GFP signal. The graph represents the proportion of time each cell spent with its CEN1's either off-center/fused or with split sister chromatids ($n \geq 15$). Representative pictures of the different configurations are shown on the right. The blue arrows represent the SPBs. The yellow asterisks represent split *CEN1*s, the pink asterisk represents a fused *CEN1*, and the green plus sign represents the split of *CEN1* sister chromatids. **$p < 0.01$ (Student's *t* test).

DISCUSSION

Previous work has shown that Mps1 is essential for chromosome segregation in meiosis (Straight *et al.*, 2000; Poss *et al.*, 2004; Gilliland *et al.*, 2005). In budding yeast, Mps1 is critical for promoting the force-generating kMT attachments that support poleward migration of the chromosomes in meiosis I (Meyer *et al.*, 2013). But it is unclear what steps in forming, maintaining, or regulating these attachments require Mps1.

Because Dam1 is a known substrate of Mps1, we tested whether the catastrophic meiotic defects displayed by *mps1* mutants are due to a failure in phosphorylating Dam1. In mutants in which Dam1 cannot be phosphorylated by Mps1 on serines 218 and 221, mitotic kinetochores show reduced colocalization with microtubule plus-ends, leading to the model that phosphorylation of Dam1 by Mps1 is required for the conversion of low affinity plus-end microtubule attachments to high-affinity attachments (Shimogawa *et al.*, 2006). This work provides three new observations that support the notion that phosphorylation of Dam1 by Mps1 is not necessary for the formation of kinetochore attachments to microtubule plus-ends but rather to sustain those attachments. First, in *dam1-2A* mutants, the maximal velocity of minus-end directed movements is indistinguishable from that seen in wild-type controls. Second, in *dam1-2A* mutants, the inefficiency in poleward movement is not due to reduced velocity but instead is due to frequent pausing during the poleward migration. Because we measured the movement of kinetochores on intact spindles, we were not able resolve the individual microtubules to which our marked kinetochores were attached. Thus, we could not distinguish whether the pauses in *dam1-2A* cells were due to a failure to retain plus-end attachments or to pauses or reversals of microtubule depolymerization (Figure 7A). This second possibility is consistent with the finding that in mitotic *dam1-2A* mutants the microtubule plus-ends are often not colocalized with kinetochores and the microtubules are longer than in wild-type cells, leading to the suggestion that Dam1 phosphorylation affects the dynamics of kinetochore microtubules (Shimogawa *et al.*, 2006). Third, in *dam1-2A* mutants, the stretched-apart centromeres of bioriented chromosomes frequently snap together, coupled with a collapse of the bivalent to one pole. This behavior is consistent with a failure to maintain kMT connections under tension. Together these observations suggest that *dam1-2A* mutants can form plus-end kMT attachments that support maximal rapid poleward movement but cannot maintain those attachments.

The failure of *mps1* mutants to phosphorylate Dam1 does not explain the massive defects in meiotic chromosome segregation exhibited by *mps1* mutants. Despite their defects in kMT interactions, *dam1-2A* mutants exhibit rather mild meiotic chromosome segregation defects, just as has been reported for mitotic cells (Shimogawa *et al.*, 2006). Consistent with this, expression of *DAM1* phosphomimetic alleles could only modestly improve the very high meiotic error-rate of *mps1* mutants. Thus, there must be another role (or roles) of Mps1 that explains its essentiality for meiotic chromosome segregation. Further work is required to identify these Mps1 substrates that are essential for meiotic chromosome biorientation.

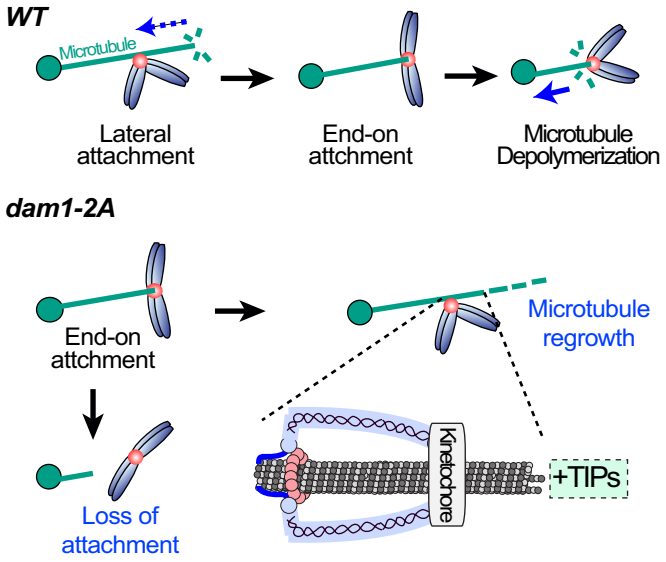

FIGURE 7: Models illustrating function of Mps1 and Dam1 and the difference between mitosis and meiosis. In wild-type cells, kinetochores (red circle) originally attach laterally to microtubule before being converted to an end-on attachment to the plus end of the microtubule. We hypothesize that in *dam1-2A* mutants either end-on attachments are unstable, or the microtubules more often regrow, separating the plus-end from the kinetochore.

MATERIALS AND METHODS

Yeast strains and culture conditions

All strains are derivatives of two strains termed X and Y described previously (Dresser *et al.*, 1994). We used standard yeast culture methods (Burke *et al.*, 2000). To induce meiosis, cells were grown in YP acetate to (4–4.5) × 10^7 cells/ ml and then shifted to 1% potassium acetate at 10^8 cells/ml. The inhibitor of Mps1-as1, 1NM-PP1, was added when indicated at 10 μM.

Genome modifications

Heterozygous and homozygous CEN1-GFP dots. An array of 256 lacO operator sites on plasmid pJN2 was integrated near the *CEN1* locus (coordinates 153583–154854). *lacI-GFP* fusions under the control of P_{CYC1} and P_{DMC1} were also expressed in this strain to visualize the location of the *lacO* operator sites during meiosis as described in Meyer *et al.* (2013).

Gene modifications. PCR-based methods were used to create complete deletions of ORFs (*spo11::HIS3MX6, mad2::NATMX6)* and promoter insertions (*natNT2::*P_{GAL1}*-NDT80, KANMX::*P_{GAL1}*-NDT80*) (Longtine *et al.*, 1998; Janke *et al.*, 2004). *spo11::KANMX,* P_{GPD1}*-GAL4(848)-ERURA3::hphNT1,* P_{HIS3}*-GFP-TUB1-URA3, mps1::KANMX, TRP1::10Xmyc-mps1-as1 (=mps1-as1), KANMX::*P_{CLB2}*-3HA-MPS1 (=mps1-md), KANMX::*P_{CLB2}*-3HA-NDC80 (=ndc80-md), SPC42-DsRed-URA3* strains were generated previously (Meyer *et al.*, 2013). The *SPC42-GFP-TRP1* strain was a gift from Mike Dresser (Oklahoma Medical Research Foundation) (as described in Adams and Kilmartin, 1999).

dam1-2A and dam1-2D. The *dam1-2A::HIS3MX6* allele was generated by using the plasmid pMS6 (a gift from Trisha Davis [University of Washington]; see Shimogawa *et al.*, 2006). Two-step gene replacement was used to substitute the endogenous *DAM1* by *dam1-S218A S221A (dam1-2A).* A PCR-based method was used later to insert, downstream of the *dam1-2A* locus (70 base pairs after the stop codon), a phenotypic marker (*HIS3MX6*) to follow this allele: The *dam1-2D* allele was generated using the plasmid pMS8 (a gift from Trisha Davis; see Shimogawa *et al.*, 2006). A two-step gene replacement was used to substitute the endogenous *DAM1* by *dam1-S218A S221A (dam1-2D).*

dam1-md. P_{CLB2}*-3HA-DAM1* strains were constructed by use of a one-step PCR-based gene replacement method (Longtine *et al.*, 1998) with *pFA6a-*P_{CLB2}*-3HA-KanMX6* plasmid (pRK69) as the template. pRK69 plasmid was derived by replacing P_{GAL1} in *pFA6a-KanMX6-*P_{GAL1}*-3HA* with the promotor (–1 to –988) from *CLB2*, which is expressed in mitotic growth but is turned off in meiosis (Grandin and Reed, 1993).

dam1-6A-me and DAM1-me. P_{IME2}*-dam1-6A/dam1-md* (labeled "*dam1-6A-me*" in the figures) diploid strains were generated by replacing the endogenous *DAM1* by P_{IME2}*-dam1-6A* in the diploid O618 (*dam1-md/+*). The transformation was done with the digested plasmid OPL284 (p*TRP1-*P_{IME2}*-dam1-6A* cut by *SalI* and *HpaI*). P_{IME2}*-DAM1/dam1-md* (*DAM1-me)* diploid strains were generated by replacing the endogenous *DAM1* by P_{IME2}*-DAM1* in the diploid O619 (*dam1-md/DAM1*). The transformation was done with the PCR product (OPR167-1161 with OPL284 as a template). Both transformations were done in diploid strains as the expression of Dam1 is restricted to meiosis with the *IME2* promoter and will not allow cell survival of haploid strains.

Fluorescence microscopy

When analyzing fixed cells, images were collected using a Roper CoolSNAP HQ2 camera on a Zeiss Axio Imager 7.1 microscope. Images were processed and analyzed using Axiovision software. For analyzing chromosome behavior (lagging, nondisjunction), cells were fixed with 2% formaldehyde and stained with DAPI (4,6-diamidino-2-phenylindole, dihydrochloride) to visualize DNA. For homologue segregation assays (Figure 1, C and D, and Supplemental Figure S1A), cells were sporulated 9 h 30 min (3 h 30 min after release from pachytene arrest), and samples were taken for in situ immunofluoresence microscopy. Metaphase I cells were defined as cells with one DNA mass spanned by a meiotic spindle measuring 1–3.5 μm in length. Cells with long spindle were defined as cells with spindles measuring at least 3.5 μm. Mononucleate cells were defined as cells with a single DNA mass. Binucleate cells were defined as cells with two distinct separated DNA masses.

Long-term time-lapse microscopy. Time-lapse imaging (every 45–120 s for 3–4 h) were performed with CellAsic microfluidic flow chambers (www.cellasic.com) using Y04D plates with a flow rate of 5 psi. Images were collected with a Nikon Eclipse TE2000-E equipped with the Perfect Focus system, a Roper CoolSNAP HQ2 camera automated stage, an X-cite series 120 illuminator (EXFO) and NIS software. Images were processed and analyzed using NIS software. For time-lapse imaging following the spindle integrity using markers for microtubules (*TUB1-GFP)* and SPBs (*SPC42-DsRed)*, the intervals were every 5 min for 4 h (Supplemental Figure S1B). For the time-lapse imaging of *CEN1* movement, two different exposure programs were defined depending of the presence (*SPO11*) or absence (*spo11Δ*) of chiasmata. In the presence of chiasmata, the intervals were either every 2 min for 2 h and later every 5 min for 2 h (Figure 6 and Supplemental Figure S3). Without chiasmata, images were acquired every 45 s for 75 min followed by every 10 min for 3 h (Figures 2 and 3 and Supplemental Figure S2).

For monitoring movements of *CEN1-GFP* on monopolar spindles (side-by-side SPBs), following the release from prophase, centromeres were considered as unattached if they did not remain at a constant distance from the SPBs for at least four consecutives frames. Centromeres were considered to be attached if they stayed

at a constant distance from the SPBs for at least three consecutive frames or moved incrementally in one direction. The first event of clustering was defined after observing three consecutive frames when *CEN1-GFP* reaches a position within 0.75 µm of the SPB. Later events of clustering were defined when centromeres returned to their previous clustered position for at least one frame. Traverses (*CEN1* crossing the spindle from one pole to the other one) were counted only when the *CEN1-GFP* signal was overlapping with the SPB signal for at least one frame. homologues were considered to be bioriented when the signals for CEN1-GFP were distinctly separated. For monitoring the configuration of bivalents after the first bipolar attachment (Figure 6), centromeres were considered to be "split or fused" when the signals for *CEN1-GFP* were for at least one frame clearly separated in two masses in the middle of the spindle and/or fused for the remaining frames. The centromeres were considered to be "Off-centered/fused" when the signals for *CEN1-GFP* were overlapping with the SPBs for at least one frame and without being split.

High-speed time-lapse microscopy. Time-lapse imaging (every 2 s for 5–10 min) were collected using a Roper CoolSNAP HQ2 camera on a Zeiss Axio Imager 7.1 microscope fitted with a 100 ×, NA1.4, plan-Apo objective (Carl Zeiss MicroImaging), an X-cite series 120 illuminator (EXFO), and a BNC555 pulse generator (Berkeley Nucleonics) to synchronize camera exposure with focusing movements and illumination. Cells from sporulating cultures were concentrated, spread across polyethyleneimine-treated coverslips, and then covered with a thin 1% agarose pad to anchor the cells to the coverslip (Yumura *et al.*, 1984). The coverslip was then inverted over a silicone rubber gasket attached to a glass slide. Thru-focus images were acquired as described and then deconvolved to provide a two-dimensional projected image for each acquisition (Conchello and Dresser, 2007; Conrad *et al.*, 2008). For the analysis of centromere movements on bipolar spindles, the coordinates of the two SPBs (labeled by *SPC42-GFP*) and the centromeres (marked by *CEN1-GFP*) were defined for each interval. To separate the movement inherent to spindle rotation inside the cells and the movement of *CEN1* on the spindle, a relative position for *CEN1* and the two SPBs was assigned for each interval. For one SPB (SPB1) this position was defined as being constant as $x = 0$ and $y = 0$. For the other SPB (SPB2), the position was defined as x = distance between the SPBs in each frame and $y = 0$. Finally, the relative position of *CEN1* was determined by the distance between *CEN1* and SPB1 and the angle formed between the axis SPB1-SPB2 and SPB1-CEN1. As the acquisitions were done in two dimensions, the impact of the spindle rotating in three dimensions was corrected by assuming that the spindle length remained the same or increased over time. So for instances in which the SPB1-SPB2 distance decreased in sequential frames, the value was corrected by replacing by the SPB1-SPB2 distance with the prior maximum spindle length (dMax SPB1-SPB2). The magnitude of this correction was also then applied to correct the SPB1-CEN1 distance, and the following formula was applied for each interval: Distance SPB1-CEN1 = Observed distance SPB1-CEN1 * dMax SPB1-SPB2/observed distance SPB1-SPB2. The velocity of *CEN1* movement on the spindle was calculated for each interval by adding the distance between interval n-1 to n+1 and dividing by time the interval (4 s). The median position for *CEN1* was determined in sliding 5-min intervals for each cell by calculating the average position. The dispersion distance was determined for each interval by calculating the distance between *CEN1* and this average position. Cells with the following characteristics were selected to monitor poleward migration (Figure 5): The *CEN1* exhibited a migration of 0.9–1.2 µm to a final destination within 0.25 µm of one SPB. The angle of approach had to be within 15°C on the pole to pole spindle axis. The migrations started within the same half-spindle of the destination SPB. Inside this 0.9- to 1.2-µm-distance movement, the intermediate steps were considered poleward movement when the distance between SPB and *CEN1* from one interval to the other one was decreasing and anti-poleward movement when increasing. The pauses and reversals of direction were determined as follows. First, the distance (D) between the final SPB destination and *CEN1* was calculated for each interval (frame). Second, the average distance for each sequential pair of steps was determined. Third, sequential positions in this sliding average were compared. If the distance between the SPB and CEN1 was increasing ($D \geq 0$), then the movement was considered to be paused/reversed. The number of consecutive poleward steps was determined as the number of consecutive steps showing continued decreasing distance ($D < 0$).

ACKNOWLEDGMENTS

We thank Trisha Davis for providing *DAM1* plasmids. We thank Michael Dresser for providing OMRFQuant Imaging Software and Emma Lee for guidance in using Thru-focus Imaging methods. This project was supported by National Institutes of Health grants R01GM087377 and R01GM110271 awarded to D.S.D. L.B. and J.B. contributed to this project as participants in the OMRF Fleming Scholars Program for undergraduate summer research.

REFERENCES

Abrieu A, Magnaghi-Jaulin L, Kahana JA, Peter M, Castro A, Vigneron S, Lorca T, Cleveland DW, Labbe JC (2001). Mps1 is a kinetochore-associated kinase essential for the vertebrate mitotic checkpoint. Cell 106, 83–93.

Adams IR, Kilmartin JV (1999). Localization of core spindle pole body (SPB) components during SPB duplication in Saccharomyces cerevisiae. J Cell Biol 145, 809–823.

Aravamudhan P, Goldfarb AA, Joglekar AP (2015). The kinetochore encodes a mechanical switch to disrupt spindle assembly checkpoint signalling. Nat Cell Biol 17, 868–879.

Asbury CL, Gestaut DR, Powers AF, Franck AD, Davis TN (2006). The Dam1 kinetochore complex harnesses microtubule dynamics to produce force and movement. Proc Natl Acad Sci USA 103, 9873–9878.

Biggins S (2013). The composition, functions, and regulation of the budding yeast kinetochore. Genetics 194, 817–846.

Biggins S, Severin FF, Bhalla N, Sassoon I, Hyman AA, Murray AW (1999). The conserved protein kinase Ipl1 regulates microtubule binding to kinetochores in budding yeast. Genes Dev 13, 532–544.

Burke D, Dawson D, Stearns T (2000). Methods in Yeast Genetics, Cold Spring Harbor Laboratory Press.

Cheeseman IM, Anderson S, Jwa M, Green EM, Kang J, Yates JR 3rd, Chan CS, Drubin DG, Barnes G (2002). Phospho-regulation of kinetochore-microtubule attachments by the Aurora kinase Ipl1p. Cell 111, 163–172.

Cheslock PS, Kemp BJ, Boumil RM, Dawson DS (2005). The roles of MAD1, MAD2 and MAD3 in meiotic progression and the segregation of nonexchange chromosomes. Nat Genet 37, 756–760.

Conchello JA, Dresser ME (2007). Extended depth-of-focus microscopy via constrained deconvolution. J Biomed Opt 12, 064026.

Conrad MN, Lee CY, Chao G, Shinohara M, Kosaka H, Shinohara A, Conchello JA, Dresser ME (2008). Rapid telomere movement in meiotic prophase is promoted by NDJ1, MPS3, and CSM4 and is modulated by recombination. Cell 133, 1175–1187.

Daum JR, Wren JD, Daniel JJ, Sivakumar S, McAvoy JN, Potapova TA, Gorbsky GJ (2009). Ska3 is required for spindle checkpoint silencing and the maintenance of chromosome cohesion in mitosis. Curr Biol 19, 1467–1472.

Dresser ME, Ewing DJ, Harwell SN, Coody D, Conrad MN (1994). Nonhomologous synapsis and reduced crossing over in a heterozygous paracentric inversion in Saccharomyces cerevisiae. Genetics 138, 633–647.

Duro E, Marston AL (2015). From equator to pole: splitting chromosomes in mitosis and meiosis. Genes Dev 29, 109–122.

Etemad B, Kops GJ (2016). Attachment issues: kinetochore transformations and spindle checkpoint silencing. Curr Opin Cell Biol 39, 101–108.
Franck AD, Powers AF, Gestaut DR, Gonen T, Davis TN, Asbury CL (2007). Tension applied through the Dam1 complex promotes microtubule elongation providing a direct mechanism for length control in mitosis. Nat Cell Biol 9, 832–837.
Franco A, Meadows JC, Millar JB (2007). The Dam1/DASH complex is required for the retrieval of unclustered kinetochores in fission yeast. J Cell Sci 120, 3345–3351.
Gachet Y, Reyes C, Courtheoux T, Goldstone S, Gay G, Serrurier C, Tournier S (2008). Sister kinetochore recapture in fission yeast occurs by two distinct mechanisms, both requiring Dam1 and Klp2. Mol Biol Cell 19, 1646–1662.
Gaitanos TN, Santamaria A, Jeyaprakash AA, Wang B, Conti E, Nigg EA (2009). Stable kinetochore-microtubule interactions depend on the Ska complex and its new component Ska3/C13Orf3. EMBO J 28, 1442–1452.
Gandhi SR, Gierlinski M, Mino A, Tanaka K, Kitamura E, Clayton L, Tanaka TU (2011). Kinetochore-dependent microtubule rescue ensures their efficient and sustained interactions in early mitosis. Dev Cell 21, 920–933.
Gilliland WD, Wayson SM, Hawley RS (2005). The meiotic defects of mutants in the Drosophila mps1 gene reveal a critical role of Mps1 in the segregation of achiasmate homologs. Curr Biol 15, 672–677.
Godek KM, Kabeche L, Compton DA (2015). Regulation of kinetochore-microtubule attachments through homeostatic control during mitosis. Nat Rev Mol Cell Biol 16, 57–64.
Grandin N, Reed SI (1993). Differential function and expression of Saccharomyces cerevisiae B-type cyclins in mitosis and meiosis. Mol Cell Biol 13, 2113–2125.
Grishchuk EL, Efremov AK, Volkov VA, Spiridonov IS, Gudimchuk N, Westermann S, Drubin D, Barnes G, McIntosh JR, Ataullakhanov FI (2008). The Dam1 ring binds microtubules strongly enough to be a processive as well as energy-efficient coupler for chromosome motion. Proc Natl Acad Sci USA 105, 15423–15428.
Hardwick KG, Weiss E, Luca FC, Winey M, Murray AW (1996). Activation of the budding yeast spindle assembly checkpoint without mitotic spindle disruption. Science 273, 953–956.
Hayden JH, Bowser SS, Rieder CL (1990). Kinetochores capture astral microtubules during chromosome attachment to the mitotic spindle: direct visualization in live newt lung cells. J Cell Biol 111, 1039–1045.
Hiruma Y, Sacristan C, Pachis ST, Adamopoulos A, Kuijt T, Ubbink M, von Castelmur E, Perrakis A, Kops GJ (2015). CELL DIVISION CYCLE. Competition between MPS1 and microtubules at kinetochores regulates spindle checkpoint signaling. Science 348, 1264–1267.
Hoyt MA, Totis L, Roberts BT (1991). S. cerevisiae genes required for cell cycle arrest in response to loss of microtubule function. Cell 66, 507–517.
Janke C, Magiera MM, Rathfelder N, Taxis C, Reber S, Maekawa H, Moreno-Borchart A, Doenges G, Schwob E, Schiebel E, Knop M (2004). A versatile toolbox for PCR-based tagging of yeast genes: new fluorescent proteins, more markers and promoter substitution cassettes. Yeast 21, 947–962.
Jelluma N, Dansen TB, Sliedrecht T, Kwiatkowski NP, Kops GJ (2010). Release of Mps1 from kinetochores is crucial for timely anaphase onset. J Cell Biol 191, 281–290.
Ji Z, Gao H, Yu H (2015). Cell division cycle. Kinetochore attachment sensed by competitive Mps1 and microtubule binding to Ndc80C. Science 348, 1260–1264.
Joglekar AP (2016). A cell biological perspective on past, present and future investigations of the spindle assembly checkpoint. Biology 5, 44.
Jones MH, Bachant JB, Castillo AR, Giddings TH Jr, Winey M (1999). Yeast Dam1p is required to maintain spindle integrity during mitosis and interacts with the Mps1p kinase. Mol Biol Cell 10, 2377–2391.
Kemmler S, Stach M, Knapp M, Ortiz J, Pfannstiel J, Ruppert T, Lechner J (2009). Mimicking Ndc80 phosphorylation triggers spindle assembly checkpoint signalling. EMBO J 28, 1099–1110.
Kitamura E, Tanaka K, Kitamura Y, Tanaka TU (2007). Kinetochore microtubule interaction during S phase in Saccharomyces cerevisiae. Genes Dev 21, 3319–3330.
Lampert F, Hornung P, Westermann S (2010). The Dam1 complex confers microtubule plus end-tracking activity to the Ndc80 kinetochore complex. J Cell Biol 189, 641–649.
Lampert F, Mieck C, Alushin GM, Nogales E, Westermann S (2013). Molecular requirements for the formation of a kinetochore-microtubule interface by Dam1 and Ndc80 complexes. J Cell Biol 200, 21–30.
Lampson MA, Grishchuk EL (2017). Mechanisms to avoid and correct erroneous kinetochore-microtubule attachments. Biology 6, 1.
Lee BH, Amon A (2003). Role of Polo-like kinase CDC5 in programming meiosis I chromosome segregation. Science 300, 482–486.
Li R, Murray AW (1991). Feedback control of mitosis in budding yeast. Cell 66, 519–531.
Longtine MS, McKenzie A 3rd, Demarini DJ, Shah NG, Wach A, Brachat A, Philippsen P, Pringle JR (1998). Additional modules for versatile and economical PCR-based gene deletion and modification in Saccharomyces cerevisiae. Yeast 14, 953–961.
Maciejowski J, Drechsler H, Grundner-Culemann K, Ballister ER, Rodriguez-Rodriguez JA, Rodriguez-Bravo V, Jones MJK, Foley E, Lampson MA, Daub H, *et al.* (2017). Mps1 regulates kinetochore-microtubule attachment stability via the Ska complex to ensure error-free chromosome segregation. Dev Cell 41, 143–156e146.
Magidson V, O'Connell CB, Loncarek J, Paul R, Mogilner A, Khodjakov A (2011). The spatial arrangement of chromosomes during prometaphase facilitates spindle assembly. Cell 146, 555–567.
Merdes A, De Mey J (1990). The mechanism of kinetochore-spindle attachment and polewards movement analyzed in PtK2 cells at the prophase-prometaphase transition. Eur J Cell Biol 53, 313–325.
Meyer RE, Chuong HH, Hild M, Hansen CL, Kinter M, Dawson DS (2015). Ipl1/Aurora-B is necessary for kinetochore restructuring in meiosis I in Saccharomyces cerevisiae. Mol Biol Cell 26, 2986–3000.
Meyer RE, Kim S, Obeso D, Straight PD, Winey M, Dawson DS (2013). Mps1 and Ipl1/Aurora B act sequentially to correctly orient chromosomes on the meiotic spindle of budding yeast. Science 339, 1071–1074.
Miller MP, Unal E, Brar GA, Amon A (2012). Meiosis I chromosome segregation is established through regulation of microtubule-kinetochore interactions. eLife 1, e00117.
Nijenhuis W, von Castelmur E, Littler D, De Marco V, Tromer E, Vleugel M, van Osch MH, Snel B, Perrakis A, Kops GJ (2013). A TPR domain-containing N-terminal module of MPS1 is required for its kinetochore localization by Aurora B. J Cell Biol 201, 217–231.
Poss KD, Nechiporuk A, Stringer KF, Lee C, Keating MT (2004). Germ cell aneuploidy in zebrafish with mutations in the mitotic checkpoint gene mps1. Genes Dev 18, 1527–1532.
Powers AF, Franck AD, Gestaut DR, Cooper J, Gracyzk B, Wei RR, Wordeman L, Davis TN, Asbury CL (2009). The Ndc80 kinetochore complex forms load-bearing attachments to dynamic microtubule tips via biased diffusion. Cell 136, 865–875.
Rieder CL (1990). Formation of the astral mitotic spindle: ultrastructural basis for the centrosome-kinetochore interaction. Electron Microsc Rev 3, 269–300.
Sarangapani KK, Akiyoshi B, Duggan NM, Biggins S, Asbury CL (2013). Phosphoregulation promotes release of kinetochores from dynamic microtubules via multiple mechanisms. Proc Natl Acad Sci USA 110, 7282–7287.
Schmidt JC, Arthanari H, Boeszoermenyi A, Dashkevich NM, Wilson-Kubalek EM, Monnier N, Markus M, Oberer M, Milligan RA, Bathe M, *et al.* (2012). The kinetochore-bound Ska1 complex tracks depolymerizing microtubules and binds to curved protofilaments. Dev Cell 23, 968–980.
Shimogawa MM, Graczyk B, Gardner MK, Francis SE, White EA, Ess M, Molk JN, Ruse C, Niessen S, Yates JR 3rd, *et al.* (2006). Mps1 phosphorylation of Dam1 couples kinetochores to microtubule plus ends at metaphase. Curr Biol 16, 1489–1501.
Shimogawa MM, Wargacki MM, Muller EG, Davis TN (2010). Laterally attached kinetochores recruit the checkpoint protein Bub1, but satisfy the spindle checkpoint. Cell Cycle 9, 3619–3628.
Shonn MA, McCarroll R, Murray AW (2000). Requirement of the spindle checkpoint for proper chromosome segregation in budding yeast meiosis. Science 289, 300–303.
Straight PD, Giddings TH Jr, Winey M (2000). Mps1p regulates meiotic spindle pole body duplication in addition to having novel roles during sporulation. Mol Biol Cell 11, 3525–3537.
Tanaka K, Kitamura E, Kitamura Y, Tanaka TU (2007). Molecular mechanisms of microtubule-dependent kinetochore transport toward spindle poles. J Cell Biol 178, 269–281.
Tanaka K, Mukae N, Dewar H, van Breugel M, James EK, Prescott AR, Antony C, Tanaka TU (2005). Molecular mechanisms of kinetochore capture by spindle microtubules. Nature 434, 987–994.
Tanaka TU (2010). Kinetochore-microtubule interactions: steps towards bi-orientation. EMBO J 29, 4070–4082.
Tanaka TU, Rachidi N, Janke C, Pereira G, Galova M, Schiebel E, Stark MJ, Nasmyth K (2002). Evidence that the Ipl1-Sli15 (Aurora kinase-INCENP) complex promotes chromosome bi-orientation by altering kinetochore-spindle pole connections. Cell 108, 317–329.

Tien JF, Umbreit NT, Gestaut DR, Franck AD, Cooper J, Wordeman L, Gonen T, Asbury CL, Davis TN (2010). Cooperation of the Dam1 and Ndc80 kinetochore complexes enhances microtubule coupling and is regulated by aurora B. J Cell Biol 189, 713–723.

Umbreit NT, Miller MP, Tien JF, Ortola JC, Gui L, Lee KK, Biggins S, Asbury CL, Davis TN (2014). Kinetochores require oligomerization of Dam1 complex to maintain microtubule attachments against tension and promote biorientation. Nat Commun 5, 4951.

Volkov VA, Zaytsev AV, Gudimchuk N, Grissom PM, Gintsburg AL, Ataullakhanov FI, McIntosh JR, Grishchuk EL (2013). Long tethers provide high-force coupling of the Dam1 ring to shortening microtubules. Proc Natl Acad Sci USA 110, 7708–7713.

Weiss E, Winey M (1996). The Saccharomyces cerevisiae spindle pole body duplication gene MPS1 is part of a mitotic checkpoint. J Cell Biol 132, 111–123.

Welburn JP, Grishchuk EL, Backer CB, Wilson-Kubalek EM, Yates JR 3rd, Cheeseman IM (2009). The human kinetochore Ska1 complex facilitates microtubule depolymerization-coupled motility. Dev Cell 16, 374–385.

Westermann S, Wang HW, Avila-Sakar A, Drubin DG, Nogales E, Barnes G (2006). The Dam1 kinetochore ring complex moves processively on depolymerizing microtubule ends. Nature 440, 565–569.

Yumura S, Mori H, Fukui Y (1984). Localization of actin and myosin for the study of ameboid movement in Dictyostelium using improved immunofluorescence. J Cell Biol 99, 894–899.

Zelter A, Bonomi M, Kim J, Umbreit NT, Hoopmann MR, Johnson R, Riffle M, Jaschob D, MacCoss MJ, Moritz RL, Davis TN (2015). The molecular architecture of the Dam1 kinetochore complex is defined by cross-linking based structural modelling. Nat Commun 6, 8673.